Performance of the Load-in-the-Loop Single Op-Amp Voltage Controlled Current Source from the Op-Amp Parameters

R Macías[1,2], F Seoane[2,3] and R Bragós[1]

[1] Department of Electronic Engineering, Universitat Politècnica de Catalunya. Campus Nord, C-4. Jordi Girona 1-3. 08034, Barcelona. SPAIN

[2] School of Engineering, University of Borås, SE-501 90 Borås, SWEDEN

[3] Department of Signal and Systems, Chalmers University of Technology, SE-41296, Gothenburg, SWEDEN

E-mail: rbb@eel.upc.edu

Abstract. In recent years, Electrical Bioimpedance (EBI) methods have gained importance. These methods are often based on obtaining impedance spectrum in the range of β-dispersion, *i.e. from a few kHz up to some MHz*. To measure EBI a constant current is often injected and the voltage across the tissue under study is recorded. Due to the performance of the current source influences the performance of the entire system, in terms of frequency range, several designs have been implemented and studied. In this paper the basic structure of a Voltage-Controlled Current Source based on a single Op-Amp in inverter configuration with a floating load, known as load-in-the-loop current source, is revisited and studied deeply. We focus on the dependence of the output impedance with the circuit parameters, *i.e. the feedback resistor and the inverter-input resistor*, and the Op-Amp main parameters, *i.e. open loop gain, CMRR and input impedance*. After obtaining the experimental results, using modern Op-Amps, and comparing to the theoretical and simulated ones, they confirm the design under study can be a good solution for multi-frequency wideband EBI applications because of higher values of the output impedance than 100kΩ at 1MHz are obtained. Furthermore, an enhancement of the basic design, using a current conveyor as a first stage, is proposed, studied and implemented.

1. Introduction

Given the number of applications of wideband EBI spectroscopy arisen recently in several medical fields such as skin cancer detection [1] or organ transplantation [2], researching and developing new EBI measurement systems with the upper limit frequency as high as possible is required. Hence and due to the current source is an essential block of these systems, several more complex approaches have been proposed aiming to improve their performances in terms of frequency range. Unfortunately, the performance of all these complex approaches degrades markedly near or below 1MHz.

On the other hand, advances in the development of integrated circuits have provided new wide-bandwidth Op-Amps. Therefore, in this paper a simple structure based on a simple, single Op-Amp based circuit topology to operate as a Voltage-Controlled Current Source (VCCS) in wide-bandwidth EBI applications is revisited. Furthermore, an enhancement of this structure is also proposed, studied and tested.

2. Theoretical Analysis

As previously mentioned, current sources are an essential block of EBI systems. Ideally, a current source generates an electrical signal with constant current amplitude independently of the load at any frequency. That means the value of the output impedance, Z_{out}, must be infinite at all frequencies [3]. In practice, the value of the Z_{out} is not infinite and it is frequency-dependent. Therefore, the main aim is to achieve current sources with a large output impedance value for a frequency range as wide as possible.

Thus, in this section the output current, I_{out}, and the output impedance of both structures are obtained mathematically and their dependences in terms of several parameters are studied. The first structure is a basic structure based on a single Op-Amp in inverting configuration with floating load, also known as load-in-the-loop current source [4]; see figure 1. The other is based on an enhancement of the first one. It consists of adding a first stage based on a VCCS implemented by a current conveyor (CCII) [4]; see figure 2.

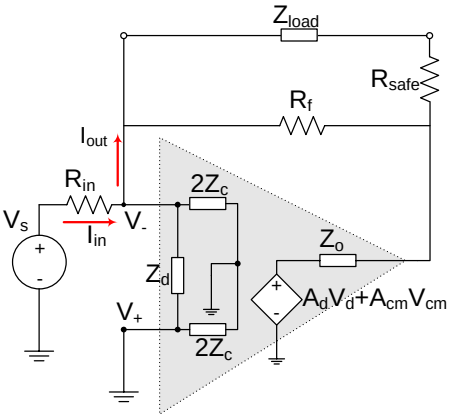

Figure 1. Load-in-the-Loop Current Source.

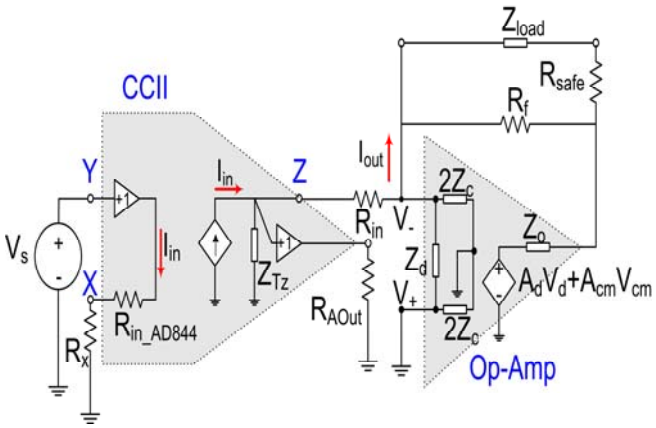

Figure 2. Current-Driven VCCS. It consists of the Load-in-the-Loop Current source driven by a CCII.

2.1. A Single Op-Amp VCCS: Load-in-the-Loop Current Source

To carry out a detailed and realistic analysis of the circuit, a non-ideal operational model of Op-Amp has been selected. It takes into account a finite value of the differential and common-mode input impedance, Z_d and Z_c respectively, a non-zero output impedance, Z_o, and a non-zero common-mode gain, A_{cm}. Furthermore, it also considers the differential-mode gain and the common-mode rejection ratio are frequency-dependent, $A_d(s)$ and $CMRR(s)$ respectively.
Therefore, given the aforementioned considerations, the circuit under study can be analyzed.

2.1.1. The output current, I_{out}. It is given by the ratio between V_s and R_{in}; see (1). R_{in} is then the transconductance of the Load-in-the-loop current source.

$$I_{out} \approx I_{in} = \frac{V_s}{R_{in}} \tag{1}$$

2.1.2. The ouput impedance, $Z_{out}(s)$. To find the output impedance of the circuit, the voltage source, V_s, and the load, Z_{load}, are replaced for a short circuit and an auxiliary voltage source, V_x, respectively. Furthermore, the overall input impedance of the Op-Amp, Z_{in}, can be written as (2). Therefore, given the simplified circuit shown in figure 3, the expression for the output impedance can be written as (3),

$$Z_{in} = \left(Z_d \left\| 2Z_c \right. \right) \tag{2}$$

$$Z_{out}(s) = R_{safe} + R_f \left\| \left(Z_o + \left(R_{in} \| Z_{in} \right) \cdot opz(s) \right) \right. \tag{3}$$

where *opz(s)* is the Op-Amp Impedance factor and is defined as (4).

$$opz(s) = 1 + A_d(s) \cdot \left(1 - \frac{1}{2CMRR(s)} \right) \tag{4}$$

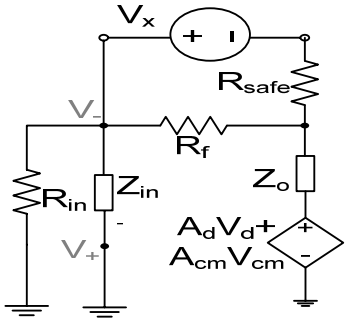

Figure 3. Equivalent circuit used to calculate the output impedance of the Load-in-the-Loop Current Source.

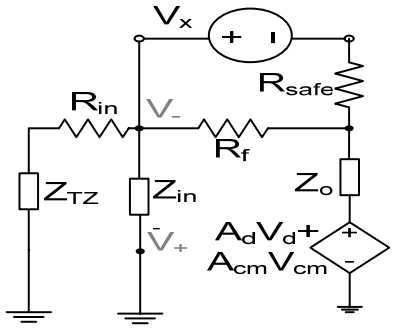

Figure 4. Equivalent circuit used to calculate the output impedance of the Current-Driven VCCS.

2.2. Current-Driven VCCS

The second proposed circuit consists basically on replacing the Thevenin source, V_s, by a Norton source, *i.e. the CCII shown in figure 2*. Thus, the output current, I_{out}, is generated independently of any element related to $Z_{out}(s)$. Furthermore, the output impedance of this circuit is essentially proportional to the features of the active devices instead of the input resistor, R_{in}. This allows to overcome the intrinsic limitation posed by the fact that R_{in} cannot be arbitrarily high given that it defines the transconductance of the VCCS.

2.2.1. The output current, I_{out}. It is approximately equal to the output current in node Z of the CCII; see figure 2. Therefore, it is the same current flowing through node X [5] and it is independent of the input resistor, R_{in}; see (5).

$$I_{out} \approx I_Z = I_{in} = \frac{V_s}{R_X + R_{in\_AD844}} \tag{5}$$

2.2.2. The output impedance, $Z_{out}(s)$. After simplifying the proposed circuit into the circuit shown in figure 4, the expression for the output impedance, $Z_{out}(s)$, can be written as (6)

$$Z_{out}(s) = R_{safe} + R_f \left\| \left(Z_o + \left(\left(R_{in} + Z_{TZ} \right) \| Z_{in} \right) \cdot opz(s) \right) \right. \tag{6}$$

where Z_{TZ} is the output impedance of the CCII and its value is much higher than the input resistor, R_{in}.

3. Measurements and Results

To measure the output impedance of both configurations the Impedance Analyzer LCR HP4192A is used in Gain/Phase measurement mode and the technique used by Bertemes-Filho [6] is applied.

On the other hand, the integrated circuits used as the Op-Amp and the CCII are, respectively, LMH6654 by National Semiconductor and AD844 by Analog Devices. Furthermore, the values used for calculating the output impedance magnitude are shown in Table 1.

Table 1: Values & Expressions used for calculating the Z_{out} magnitude.

Symbol	Expression	Values		Symbol	Values
Z_d	R_{id} // C_{id}	R_{id} = 20kΩ	C_{id} = 0.55pF	Z_o	80Ω
Z_c	R_{cm} // C_{cm}	R_{cm} = 4MΩ	C_{cm} = 0.9pF	R_{in}	6.2kΩ
$A_d(s)$	$A_{d0}/(1+(s/\omega_d))$	A_{d0} = 67dB	$\omega_d = 2\pi \cdot 125$kHz	R_{safe}	390Ω
CMRR(s)	$CMRR_0/(1+(s/\omega_{cm}))$	$CMRR_0$ = 90dB	$\omega_{cm} = 2\pi \cdot 9$kHz	R_f	390kΩ
Z_{TZ}	R_{TZ} // C_{TZ}	R_{TZ} = 3MΩ	C_{TZ} = 4.5pF		

Therefore, the measured output impedance values from the experimental tests are shown in figure 5 and figure 6.

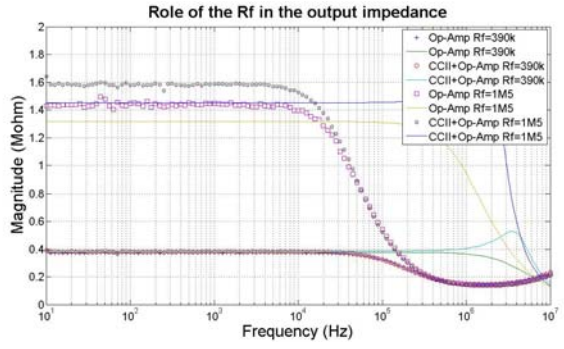

Figure 5. Plotted output impedance for different values of R_f. R_f = 390kΩ and 1.5MΩ. **N.B.** R_{in} = 6.2kΩ.

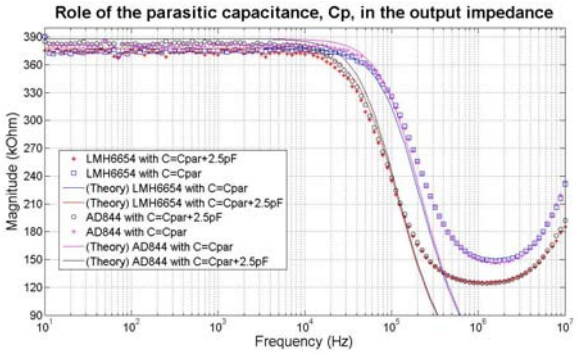

Figure 6. Adding a 2.5pF parasitic capacitance in the calculated Z_{out}, the measured and the simulated Z_{out} match up. Furthermore, if a 2.5pF capacitor is added to the implemented board, the cut-off frequency becomes smaller.

4. Discussion

4.1. Regarding the feedback resistor, R_f

Due to R_f is in parallel with the output of the current source, it acts as current divider of the output current. Furthermore, it limits the maximum value of the output impedance; see figure 5.

Thus, the higher R_f is, the higher the output impedance becomes. But, because of providing a path for the bias current of the Op-Amp is usually required in EBI systems, R_f cannot be removed.

4.2. Regarding the parasitic capacitance, C_p

As figure 5 shows, there is a good agreement between the measured and the calculated output impedance in the frequency range below 100 kHz. Above this range, the value of the cut-off frequency varies depending on the value of R_f. The higher R_f is, the smaller the cut-off frequency becomes. The main reason is because of the influence of parasitic capacitances, C_p, is not negligible at high frequencies. A 2.5pF value of C_p is found as the best value which fits with the measured output impedance.

Hence, the working frequency range for a VCCS is not given only by the Op-Amp features but also by the parasitic capacitances present at the output of the VCCS.

5. Conclusions

As this results show, implementing wideband current sources using a single Op-Amp circuit for spectroscopy measurements of EBI is a realistic approach. Using the Load-in-the-loop Current Source, wideband multifrequency applications can be implemented properly in terms of large output impedance at a very low cost. Furthermore, to achieve an output current of the VCCS more robust and constant and also independent of any element related to the output impedance, the improved circuit called Current-Driven VCCS is proposed.

Therefore, the overall output impedance for both configurations can be plotted as in figure 7. As observed, the overall output impedance is modeled as three impedances building up a parallel bridge: the Z_{in}, Z_i and R_f. The parameter Z_{in} was defined in (2) as the Op-Amp input impedance. Z_i is the equivalent input impedance from the inverting input of the Op-Amp to ground, *i.e.* R_{in} *in the Load-in-the-loop Current Source and* $R_{in}+Z_{TZ}$ *in the Current-Driven VCCS*. Furthermore, the *opz(s)* was also defined in (4) as the Op-Amp Impedance factor. The higher these three impedances and the *opz(s)* are, the higher the overall output impedance becomes. This can help to choose the right Op-Amp from the system requirements.

On the other hand, as previously mentioned, the effect of the parasitic capacitances is the critical factor limiting the performance of the current source at high frequencies. Hence, to improve the performance of the current source, parasitic capacitances should be avoided or minimized as far as possible from the earliest stage of the circuit design. Furthermore, in a real measurement system, a higher capacitance exists due to the coaxial cables connected between the current source and the load. This problem affects all current source structures and can be only overcome if the VCCS is placed near the electrodes or driven guards are used for the coaxial cables. Also dominant pole strategies can be employed to avoid oscillations in that last case.

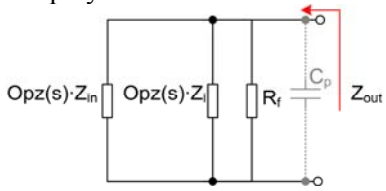

Figure 7. Equivalent circuit for the output impedance of both VCCS circuits. The parasitic capacitances' effect is added in discontinuous trace. **N.B.** the values of R_{safe} and Z_o are considered negligible.

References

[1] Aberg P, Nicander I, Hanson J, Geladi P, Holmgren U and Ollmar S 2004 Skin cancer identification using multifrequency electrical impedance – A potential screening tool. *IEEE Trans. Bio. Med. Eng.*, 51:(12), 2097-2102

[2] Ivorra A and Genesca M 2005 Bioimpedance dispersion width as a parameter to monitoring living tissues Electrical bioimpedance measurement during hypothermic rat kidney preservation for assessing ischemic injury, *In: Physiolo. Meas.*, 26:(2), 165-173

[3] Seoane F, Bragós R, Lindecrantz K and Riu P 2007 Current source design for electrical bioimpedance spectroscopy, *In: Encyclopedia of healthcare information systems*

[4] Seoane F, Bragós R and Lindecrantz K 2006 Current source for multifrequency broadband electrical bioimpedance spectroscopy systems. A novel approach. *Engineering in Medicine and Biology Society Conference, 2006. EMBS '06.* pp *5121 - 5125*

[5] Sedra S A and Roberts W G 1990 Current conveyor: theory and practice, *In: Analog IC Design: The Current-Mode Approach* pp 93-126

[6] Bertemes-Filho P, Brown B H and Wilson A J 2000 A comparison of modified Howland circuits as current generators with current mirror type circuits, *In: Physiological Measurement* 21:(1), 1-6